Final Report for JFSP Project 01-1-5-03

Automated Forecasting of Smoke Dispersion and Air Quality Using NASA Terra and Aqua Satellite Data (Task 5)

Principal Investigators:
Wei Min Hao and Shawn Urbanski
(406) 329-4829, surbanski@fs.fed.us

1 Executive Summary

Algorithms and techniques to inform an air quality forecasting system with near real-time satellite observations have been developed, demonstrated, and validated. These techniques are generally applicable to any air quality forecasting system, and in many cases do not depend on the particular satellite instrument chosen as the source of real time data. Validation of satellite derived fire products has been performed using ground truth provided by incident management teams; contrasting starkly with previous approaches of validation-by-simulation or by comparison with other measurements from space.

This document contains a description of the air quality forecasting system in operation at the Missoula Fire Science Laboratory. This air quality forecasting system has been steadily assimilating new techniques and algorithms as they have been developed over the past four years. Individual components as well as assemblies of components have utilized this system as a proving ground.

Technology transfer from this project is realized in multiple forms. Data products, many of which were not previously available anywhere, are made available on our prototype website. These include: fire detections, burn scar detections, emission maps, and a fuel map defined in terms of the FOFEM reference database. Software applications have been upgraded and optimized for integration with the rest of the system: the Carbon Bond IV photochemical mechanism has been added to HYSPLIT, and the FARSITE fire area simulator has been modified to work from the Linux command line. Finally, the web based publishing of four dimensional grids, as both data and as maps, is being added to the publicly available GeoTools library and GeoServer web map server.

This project has produced techniques, algorithms and software of generic utility. The burn scar algorithm has been published in a refereed journal. Data products and software applications have been made publicly available. These generic components have been assembled into an air quality forecasting system in operation at the Missoula Fire Science Laboratory. The current generation of products is the foundation and core of our ongoing work in air quality forecasting and will continually be improved over time.

2 System Overview

The major object of this report is to describe the air quality forecasting system funded by this project. This air quality forecasting system required the development of several new components as well as the validation of new and existing components. Techniques and components developed for this project center around the use of the MODIS instrument as a source of real-time information about current fire activity. These techniques are generically useful to other air quality forecasting systems which desire to use MODIS as a source of real time fire information. Likewise, the system defines a template for a generic air quality forecasting system which is capable of ingesting data from other satellite-based instruments, provided that specific components are customized for the instrument used.

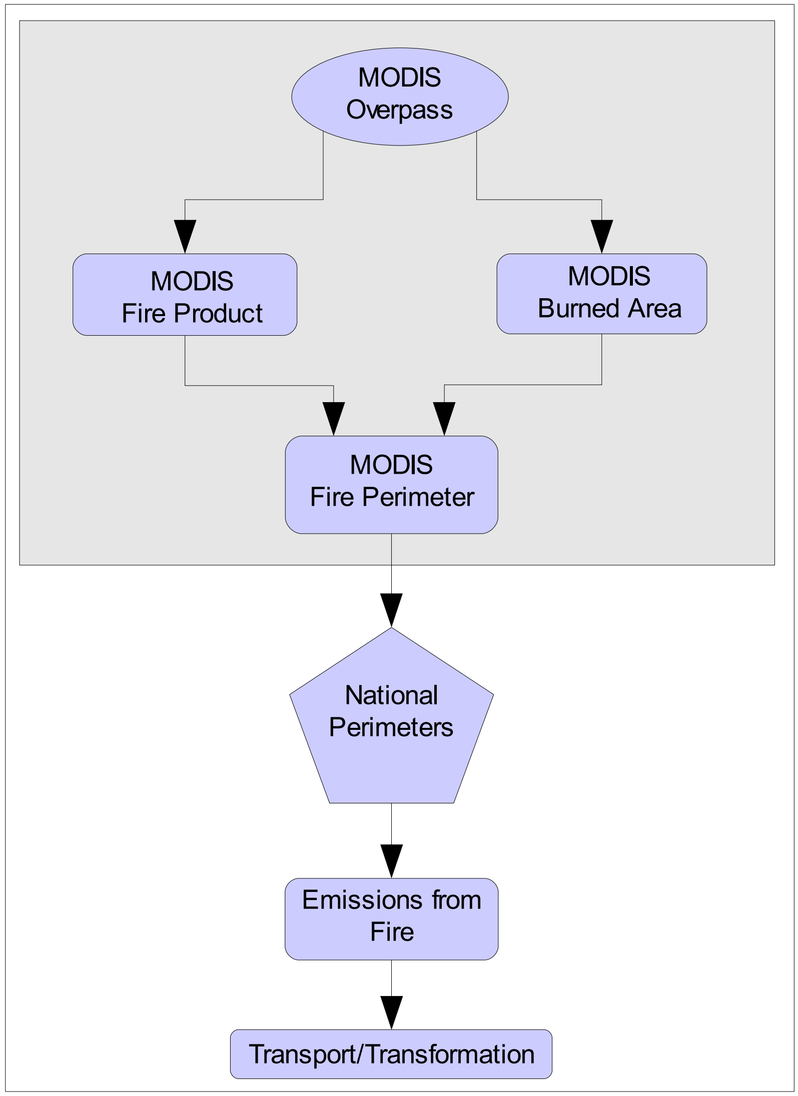

Figure 1: Logical components of the air quality forecasting system funded by this project.

The major logical components of the air quality forecasting system are depicted in Figure 1. Each of the rounded rectangles in Figure 1 represents a technique or component which has been developed or validated for use with this system. Each rounded rectangle is described in a separate section of this report.

In addition to enumerating the major logical components of the system, Figure 1 also depicts the two mutually independent time scales which will be part of any air quality forecasting system initialized from a polar orbiting satellite. In the box at the top of the figure are all the components which operate on the satellite data as the data are acquired. All of these operations are inherently subject to the properties of the satellite instrumentation used to produce the data; in this case, MODIS. These data items contain only those data which are simultaneously observable by MODIS, determined by MODIS' field of view. The pentagon labeled “National Perimeters” performs a twice-daily aggregation of the individual MODIS observations into a national fire perimeter data set. All of the system components after this aggregation operate on a daily time scale which is not tightly coupled to the particular times of satellite data acquisition.

Finally, the oval labeled “MODIS Overpass” at the top of Figure 1 indicates that the system must have access to real time or near real time satellite data. This oval represents a capital investment in a commercial off the shelf satellite ground station capable of receiving, decoding, and processing MODIS data which is transmitted in direct broadcast mode. This is a thoroughly understood enabling technology which will not be discussed further.

The remainder of this report is organized around the system components depicted as rounded rectangles in Figure 1. Each component is described in a separate section, as indicated in Table 1.

Logical Component	Section	Page
MODIS Fire Product	3	3
MODIS Burn Scar	4	6
MODIS Fire Perimeter	5	10
Emissions from Fire	6	11
Transport/Transformation	7	14

Table 1: Air quality modeling components described in this final report.

3 Validation of MODIS Fire and Thermal Anomaly Product

The MODIS Fire and Thermal Anomaly product is one of the standard products generated by NASA from all MODIS observations. NASA and UMD provide access to the global fire and thermal anomaly product data via shapefiles which are updated once daily (and the source satellite image is not provided). The algorithm has been well documented by the MODIS science team and a standardized implementation in C has been released. This code is compatible with the data files obtained from a MODIS ground station. Applying this code to the data obtained from a MODIS ground station can yield a MODIS Fire and Thermal Anomaly product within 45 minutes of the observation.

While the theoretical basis for the current algorithm is well documented [2], and has a long history of incremental improvements ([3] and [4]), this project funded the first validation using ground truth from specific, known large fires. Previous validations were conducted via simulation and by comparison with higher resolution data collected from space. This validation was conducted on specific large fires, performing a daily comparison of the area generated by traditional methods with area predicted by the fire algorithm. Calculation of the cumulative, non-overlapping area of MODIS hotspot detections for a specific incident was considered to be the measurement of area yielded by the fire algorithm.

The results of this validation are plotted in Figure 2. The linear regression which includes all four fires appears to be an extremely good fit to the data, with an R^2 of 0.93. However, closer examination of the data reveals that each fire produced a slightly different relationship of area as reported by the incident management team (IMT) to area as measured by MODIS. Separate linear regressions are warranted where each regression uses only the data from a single incident. This set of regression parameters are summarized in Table 2.

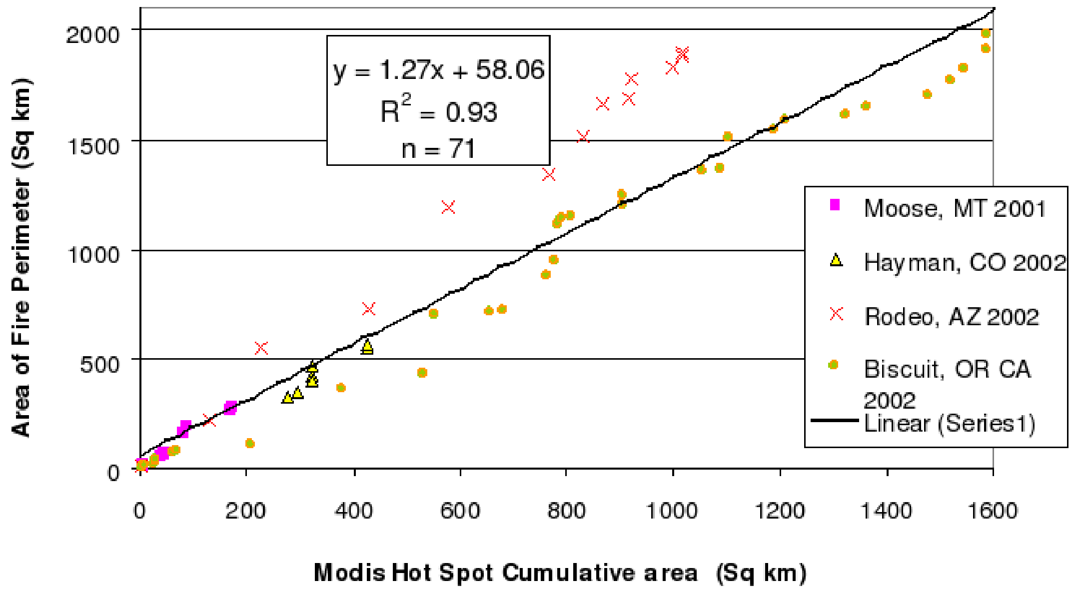

Figure 2: Comparison of area derived from incident management team fire perimeters and accumulated MODIS hotspots

Fire	Slope	Intercept	R^2	n
Rodeo	1.8495	12.895	0.9907	13
Hayman	1.5850	103.66	0.9321	7
Moose	1.723	3.159	0.9586	9
Biscuit	1.266	33.048	0.9881	42

Table 2: Summary of linear regression parameters for individual fires.

The reasons for the discrepancy in the linear regression results is not well understood. Possibilities include a difference in measurement techniques by the incident management teams and differences between how the diurnal cycle of fire activity interacts with the time of MODIS overpasses. In the end, each incident possesses a unique ratio of satellite observed fire activity to total fire activity. This ratio is visualized in figures 3 and 4 for the Rodeo and Hayman fires, respectively. As shown, the Hayman fire has a greater percentage of area which was burning at the time of the MODIS overpasses. The area reported by the IMT on the Rodeo fire includes significant expanses which were not reported as fires by MODIS.

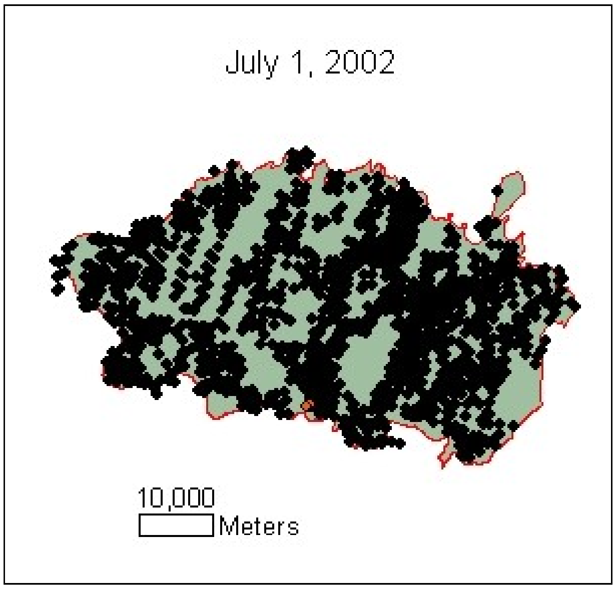

Figure 3: Final perimeter of the Rodeo Fire

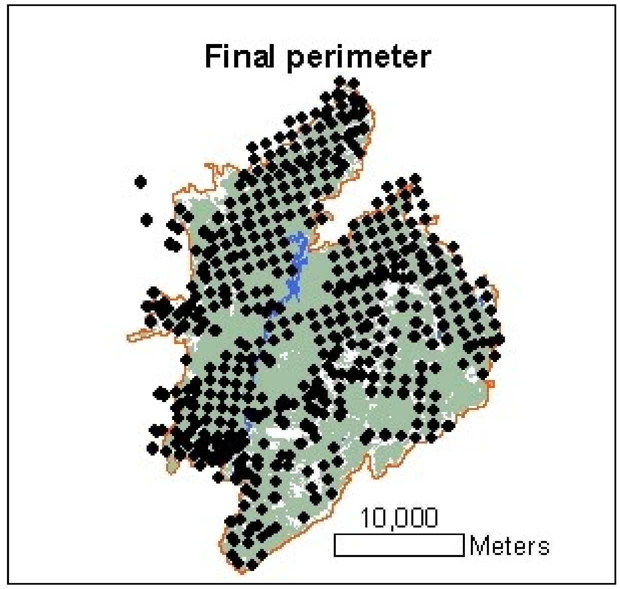

Figure 4: Final perimeter of the Hayman Fire

This validation explored the utility of area measurements obtained by accumulating MODIS hotspots. This method of area measurement was found to yield generally acceptable results for the four fires under test. The shortcomings of this method do not appear to be associated with the physics of the fire detection algorithm itself, but rather with the sampling frequency associated with a polar orbiting satellite. To predict area using an accumulation of MODIS fire detections, the equation in Figure 2 is used.

A more general validation of the fire detection algorithm was performed using a manually assembled database of ICS 209 reports. This database had entries from a variety of agencies. Double-reporting of the same fire by multiple agencies was accounted for, and duplicate entries were removed. This validation included many more fires than the detailed examination of specific large fires described above.

This more general validation is summarized in Figure 5. The validation demonstrated that the MODIS fire detection algorithm detects 80% of all fires over 300 acres (1.21 km^2). MODIS also reported fire detections which had no corresponding entry in the database used as ground truth. These are classified as "excluded fires or false alarms" because there is no way to distinguish the two cases. Of these points which MODIS reports and the database lacks, 99% occur on grasslands or agricultural areas, where the database is expected to lack information.

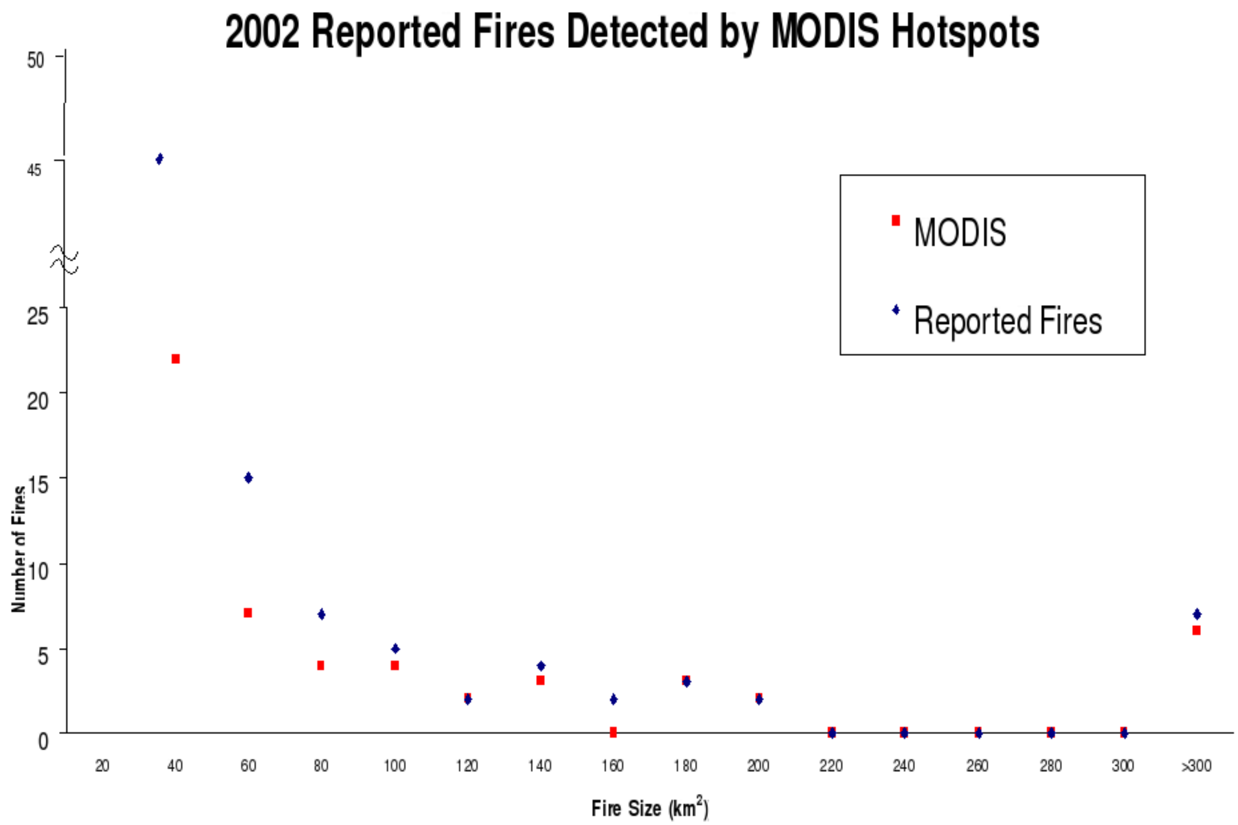

Figure 5: Validation of the MODIS fire detection algorithm against a collection of ICS-209 reports.

4 Development of a MODIS Burned Area Product

This project funded the development of a unique real-time burned area product, which has been published in the peer-reviewed literature[5]. Previously existing burned area products, such as those in use by the Burned Area Emergency Rehabilitation (BAER) teams, require two cloud free images of the burned area. The method introduced in [5] requires only one image and is capable of penetrating thin layers of smoke.

Detection and processing of burned area comprises a critical component of the air quality forecasting system. Two MODIS instruments on two spacecrafts produce four daily observations of any specific fire incident. As illustrated in the previous section, the fire algorithm is capable of detecting only what is burning at the time of the observation. Burned area information contributes a knowledge of fire activity between observations. This knowledge is necessary to determine whether the fire detections in two sequential MODIS scenes represent the advance of a flaming front or a new fire start. It also provides information about the interior structure of the perimeter: are the gaps unburned islands or did they burn between MODIS observations?

4.1 Summary of the published method

The method of burn scar detection developed for this project is presented in Equations 1-5. This method consists of a series of threshold tests, culminating in a ratio of top of the atmosphere apparent reflectance in the 1.24 micron and 2.13 micron bands. In the final form of the algorithm, all pixels which satisfy the conditions of Equations 1-5 are considered burned.

(1) $$0.05<\rho^{*}_{1.24\mu m}<0.2$$

(2) $\rho^*_{0.86\mu m} < 0.18$

(3) $\rho^*_{2.13\mu m} > 0.05$

(4) $0.10 \leqslant \rho^*_{1.64\mu m} < 1.0$

(5) $0 \leqslant \dfrac{\rho^*_{1.24\mu m} - 0.05}{\rho^*_{2.13\mu m}} < R_{th}$

In all equations, the variable ρ^* represents the apparent reflectance at the top of the atmosphere. The subscript indicates the center wavelength, in microns, of the band in which the reflectance value has been calculated. All of the bands utilized in this algorithm have a spatial resolution of 500 meters.

The quantity R_{th} in Equation 5 controls the threshold which determines whether a pixel is considered burned. Acceptable values for this quantity lie between 0.8 and 1.0. Higher values result in more false alarms and lower values reduce the ability to penetrate smoke. Lower values also miss more burned area. Each pixel is a mixture of many signals due to the coarse spatial resolution of MODIS; hence there is no single value of R_{th} which will perfectly separate burned and un-burned area.

The false alarm rate of Equation 5 was found to be unacceptable if applied indiscriminately to all pixels of a scene. Certain conditions were found to trigger the production of false alarms: water, cloud shadows, and clouds over water. Equations 1-4 were proposed in [5] as a first-order measure of control because they are reasonably simple, computationally efficient, and improved the false alarm rate.

4.2 Improvements using contextual information

While the proposed threshold tests improved the false alarm rate somewhat, using the algorithm operationally produced a staggeringly large number of false detections. We have investigated a two stage process flow designed to reduce the number of false detections:

1. A convolution filter has been added to remove small clusters of burn scar detections. If there are less than six detections in a 5x5 window, all detections in the window are eliminated.
2. Burn scar detections are eliminated if they are not proximal to a recent fire/thermal anomaly detection. To be retained, burn scars must be within 5km of any fire detection from the preceding 10 days.

These additional constraints are illustrated by Figure 6. The effect of criterion one is that isolated clusters of burn scar detections are removed from consideration. Criterion two takes into account the longevity of burn scars, and eliminates from consideration all detections caused by a fire which is no longer burning.

4.3 Validation

The validation of the burn scar algorithm proceeded in much the same way as the validation of the fire algorithm. This validation effort was undertaken before the contextual information was added to the algorithm. These additions are intended to eliminate spurious detections, a purpose which was served by manually selecting the validation data set from the MODIS scene.

The main advantage of using burn scars to measure area is that they do not need to be aggregated. Each new MODIS observation yields

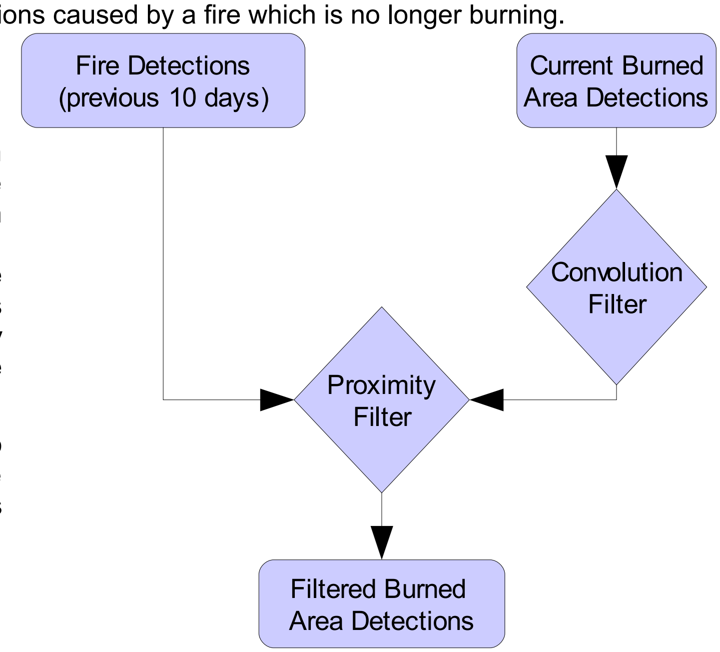

Figure 6: Contextual filtering of burned area detections.

fresh detections over the entire recently burned area. This also implies that fire activity which was not directly observed may be inferred from the set of burn scar detections. Results from this validation are presented in Figure 7.

Data from all fires participated in the production of the regression line, which has an R^2 of 0.88. The striking difference between measuring areas with this method and with the fire detection algorithm is that the most significant variation is no longer between fire events, but rather *within* individual fire events. This difference may be correlated to obscuration by smoke and clouds instead of an interaction between fire activity and observation time. As with the fire detection data, the regressions for individual fires are presented in Table 3.

In all fire events, the data exhibit the following pattern: perimeters from the IMT reflect major changes in area before the corresponding change is registered in the burn scar algorithm. This is understood to be an effect of obscuration by smoke and cloud. The burn scar algorithm, while having a limited ability to penetrate smoke, does require that heavy smoke disperse prior to yielding reliable detections. This weakness complements the strength of the fire detection algorithm, as the longer wavelengths used are less affected by smoke.

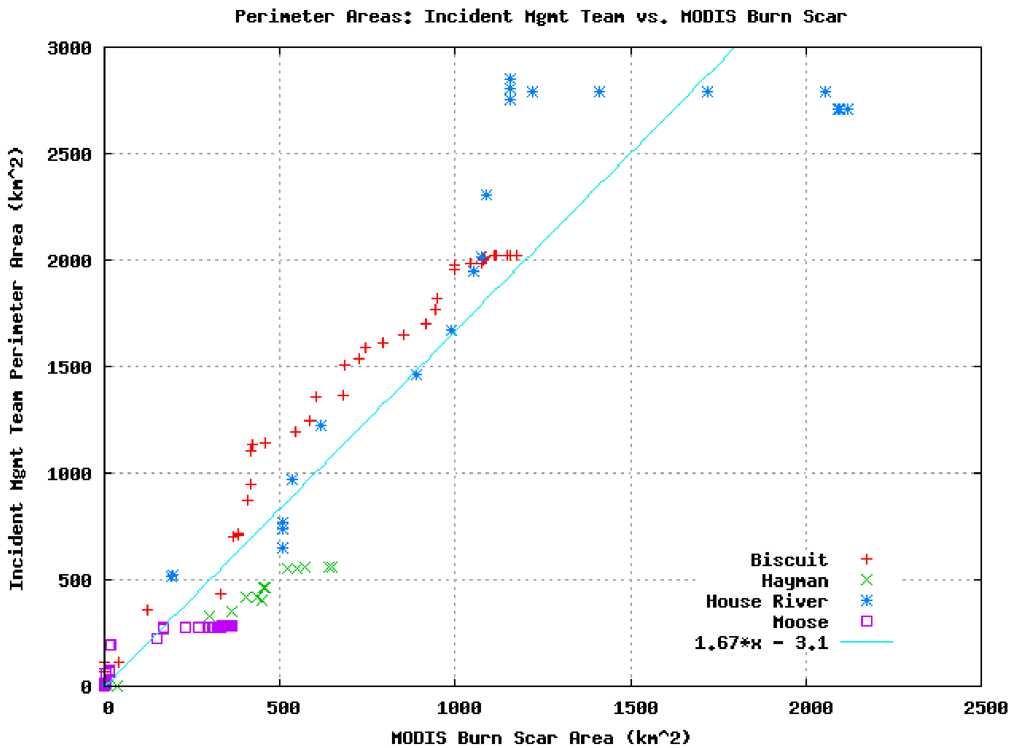

Figure 7: Validation of the MODIS Burn Scar algorithm

Fire	Slope	Intercept	R^2	n
House River	1.34	422.77	0.77	26
Hayman	0.96	-2.06	0.97	16
Moose	0.71	53.36	0.77	48
Biscuit	1.72	158.55	0.97	41
ALL FIRES	1.67	-3.1	0.88	131

Table 3: Linear Regression Parameters for Individual Fires (burn scar validation)

The final burn scar and incident fire perimeter for the Rodeo fire are presented in Figure 8. Comparison with Figure 3 shows that the burn scar algorithm fills in the interior gaps present in the fire detections. As such, the burn scar algorithm may be used to infer fire activity between observations.

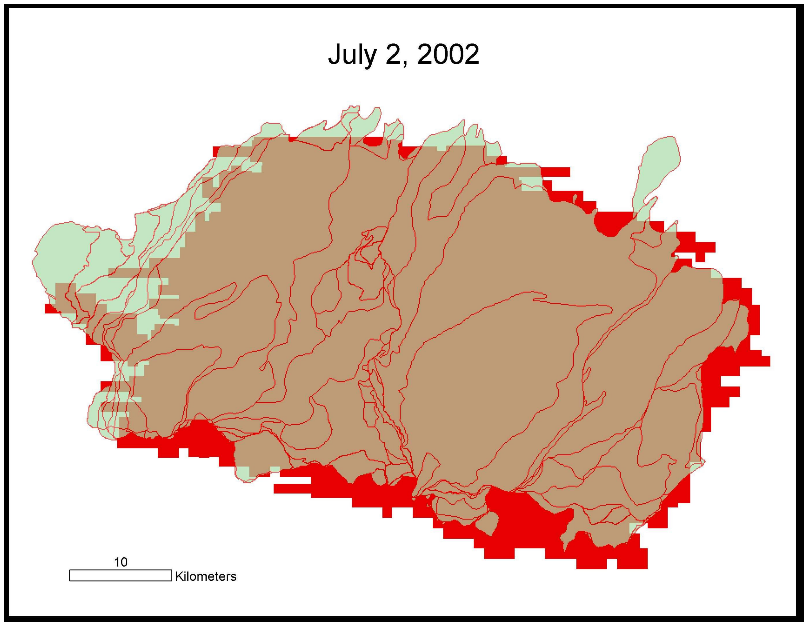

Figure 8: Final perimeter and burn scar detections for Rodeo fire. Green area is fire activity reported by the IMT. Red area represents MODIS burn scar detections. The overlap is visible due to the partially transparent nature of the IMT perimeters.

5 Perimeters from Fire and Burned Area Detections

Previous sections have demonstrated the complementary utility of the fire detection algorithm and the real time burn scar algorithm. This section describes how the two are combined to ultimately measure real-time, spatially resolved fire growth. A preliminary validation of the process is presented using the I-90 fire in Montana.

5.1 Process

The process by which fire and burn scar detections are transformed from a set of dissociated points having a continental scale to a set of "fire events" is illustrated in Figure 9. While the collection of all fire events retains a continental scale, each individual fire event has a local extent. Fire events may be produced exclusively from the data, without reference to external reporting sources. These fire events are the items which may be associated with ICS-209 and NFOD entries, although an automatic method of doing so has not been identified.

As shown in Figure 9, "current fire events", which are produced by this MODIS observation, are informed by previous runs of this algorithm on previous MODIS observations ("active fire events"). As such, the process is iterative.

In the first step, represented by "Growth and Seeding" in Figure 9, the current fire detections are added to existing fire events if they are within 5 km of an event. Fire detections which cannot be associated with an existing fire event are considered new, and a new "event" is created for them. The second step, represented by "Growth by Proximity" adds burn scar detections (which have been filtered by the process of Figure 6) within 5 km of a fire event to that event. In no case is a new fire event produced by a burn scar detection.

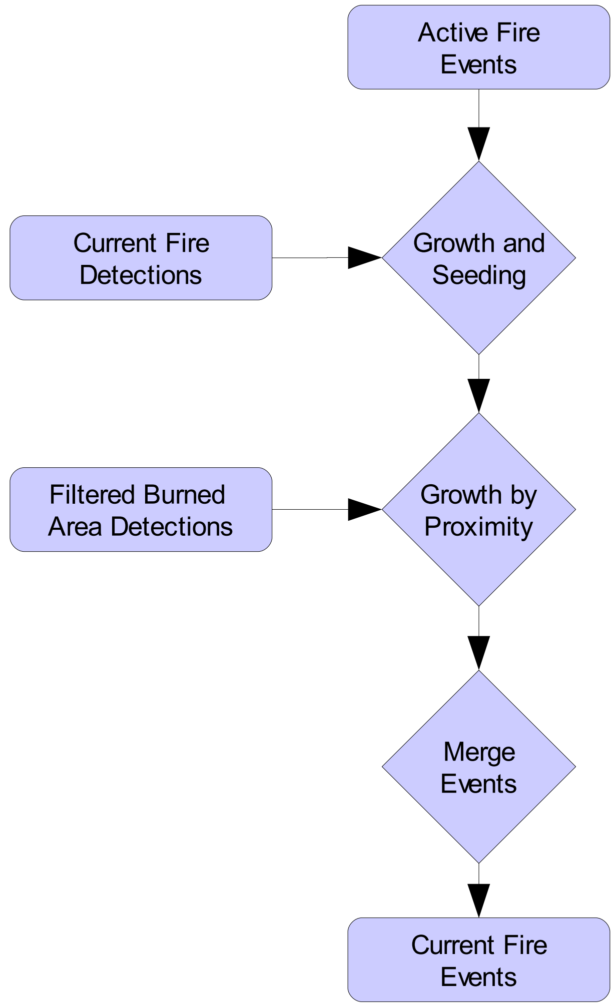

Figure 9: Process to aggregate fire and burn scar detections into "fire events".

After the fire events have accumulated new detections, a new fire event area is calculated by the process of "buffering". For each detection, a circle of an appropriate diameter (500m for burn scars, 1km for fire detections) is drawn around the center point. Using these new fire areas, the final step is to check whether two or more fire events have merged into one. Fire events are considered to have merged together if their perimeters are less than 5km apart at the point of closest approach.

Utilization of this algorithm in our operational system has caused us to modify the filtering applied to burn scars, as presented in Figure 6. In particular, the convolution filter which was put in place to remove isolated clusters of detections was found to eliminate any "fingers" or "peninsulas" present in the actual fire perimeter. Removing this filtering criterion has resulted in perimeters which replicate incident perimeters with a higher fidelity.

5.2 Demonstration

This algorithm produced the fire area shown in Figure 10 for the I-90 fire in Montana. The figure clearly shows that the fundamental unit of fire area construction is circular. It also shows the two diameters of circles used.

The small circle at the extreme northeast corner of the fire was generated from a burn scar detection and the larger circles were generated from the fire detections. All detections, fire and burn scar, are considered part of this one fire event.

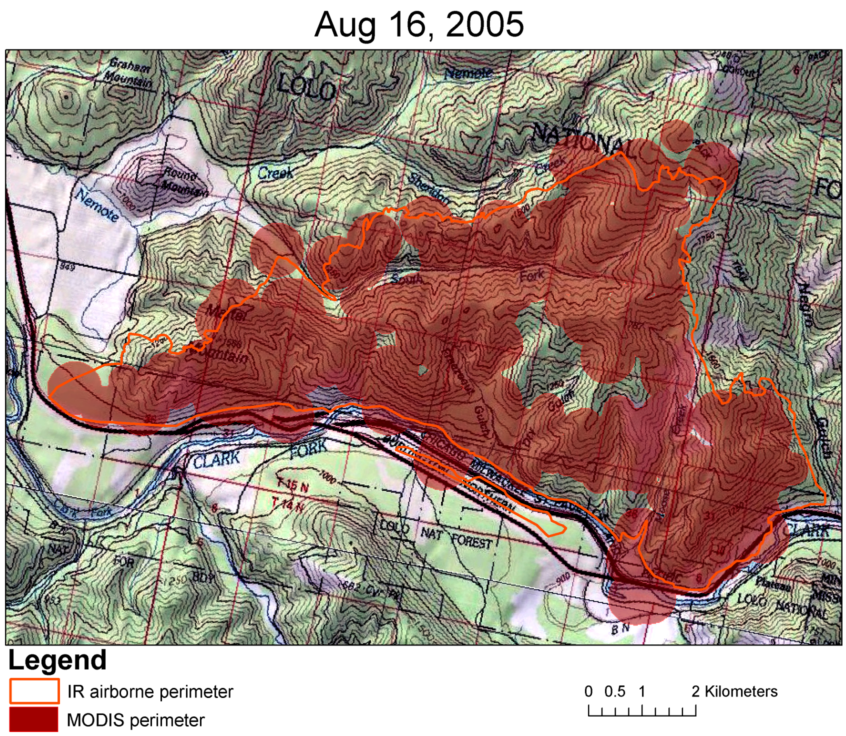

Figure 10: Demonstration of MODIS-derived fire area using the I-90 fire.

The fire area in Figure 10 also illustrates that the algorithm correctly reports unburned area interior to the fire, showing a large unburned area in the middle. Other, smaller areas which are not designated as burned represent gaps between the circles drawn around the center points of the detections. A final advantage to presenting the data as areal extents instead of points is that it provides an intuitive visual interpretation of the measurement error of the satellite. As shown, the component circles along the actively burning perimeter all enclose some portion of the airborne IR perimeter from that morning. The single exception is the burn scar point in the extreme northeast. Given the topography and the location of the fire perimeter in the morning, the perimeter could easily have advanced to the area specified by the time of the MODIS overpass.

6 Calculation of Emissions

Calculation of emissions requires knowledge of four basic quantities: area burned, fuel loadings, fuel moisture and emission factors. The work in section 5 provides a means of tracking fire area growth over time for a specified fire event. This fire area is not just a single number, it is defined by a spatially explicit perimeter. Given an appropriate fuel map, the emissions calculated from a single fire event during a burning period bounded by two satellite observations are related to the new area burned during that period *and* the fuels known to occupy that area. This powerful method is not limited to using satellite observations, but may also accept a sequence of simulated perimeters, i.e. from FARSITE. This method is also not limited to a single fire event.

The first step to calculating emissions for a burning period is to compute the new area burned in that period. For operational use when a specific fire is not targeted, our system maintains a national 1km resolution “newly burned area” grid. Each grid element is considered “burned” or “not burned”. Elements are considered newly burned when the center point of the 1km grid cell is enclosed by the total fire area (section 5) of one fire observation, but not by the total fire area of the previous observation. The times of the two observations defines the corresponding burning period.

The second critical component of an emissions calculation is knowledge of the fuel loadings. Our system uses the fuel loadings provided by the First Order Fire Effects Model (FOFEM) software. [11] Prior to this project, there was no fuel map which was directly linked to the FOFEM default fuel loadings. We have produced such a fuel map for use within our air quality forecasting system. This map has been produced using the nationwide Fuel Characteristic Classification System (FCCS) fuelbed map [6] as a source. The FCCS fuelbed map is expressed in terms of the vetted fuelbeds released with the FCCS software [10]. Part of the definition of an FCCS fuelbed is the association with one or more forest types as defined by the Society of American Foresters (SAF) [1], and/or one or more range types defined by the Society of Range Managers (SRM) [8]. It is possible to retrieve default loadings from the FOFEM reference database using SRF/SRM cover types [7]. Thus, using the FCCS fuelbed map as input a FOFEM reference database fuel map is produced, yielding a spatial characterization of fuel loadings.

Finally[1], knowledge of the specific emission factor to apply to the fuel type is required. An extensive review of the literature, as well as a thorough examination of unpublished data for the United States collected by the Fire Chemistry unit throughout the 1990s and early 2000s indicates that there are only a handful of statistically significant categories of emission factors. These categories may be roughly expressed as “forest”, “grass”, and “shrub”. The appropriate emission factor is selected based on the general category of ground cover.

These individual components are combined into a per-pixel emissions calculation using the FOFEM program. A special version of the FOFEM program has been produced. It is different from the institutional version only in that it lacks a graphical user interface and runs on the Linux command line. This special version of FOFEM executes once for every pixel, for every hour of the forecast.

This process results in a set of nationwide maps of emissions for the burning period. Depending on the quantity of interest, the pixels in this emissions map could be summed to yield emissions by fire event, by state, by region, by nation, or total emissions. Each map contains per-pixel emissions calculations for a particular chemical species tracked by the system.

6.1 Demonstration

A demonstration of the emissions calculation was performed using the Oklahoma and Texas winter fire events of 2005/6. Over 1400 km^2 (350,000 acres) of vegetation was burned from December 2005 through February 2006, as shown in Figure 11. The estimated PM2.5 (CO) fire emissions equaled ~10% (5%) of the total anthropogenic emissions (NEI 2002) in Oklahoma and Texas for the 3-month period. However, during periods of high fire activity, daily estimated fire emisisons were similar to total Oklahoma - Texas statewide anthropogenic emissions. The ratio of daily fire related emissions to anthropogenic emissions over this time period is presented in Figure 12.

These results highlight the necessity of incorporating temporally and spatially resolved fire emissions into air quality forecasting systems.

1 Fuel moistures are currently estimated using the method defined by the National Fire Danger Rating System (NFDRS). Work is in progress to inform the forecasting system with dead fuel moistures from the Wildland Fire Assessment System (WFAS) [9].

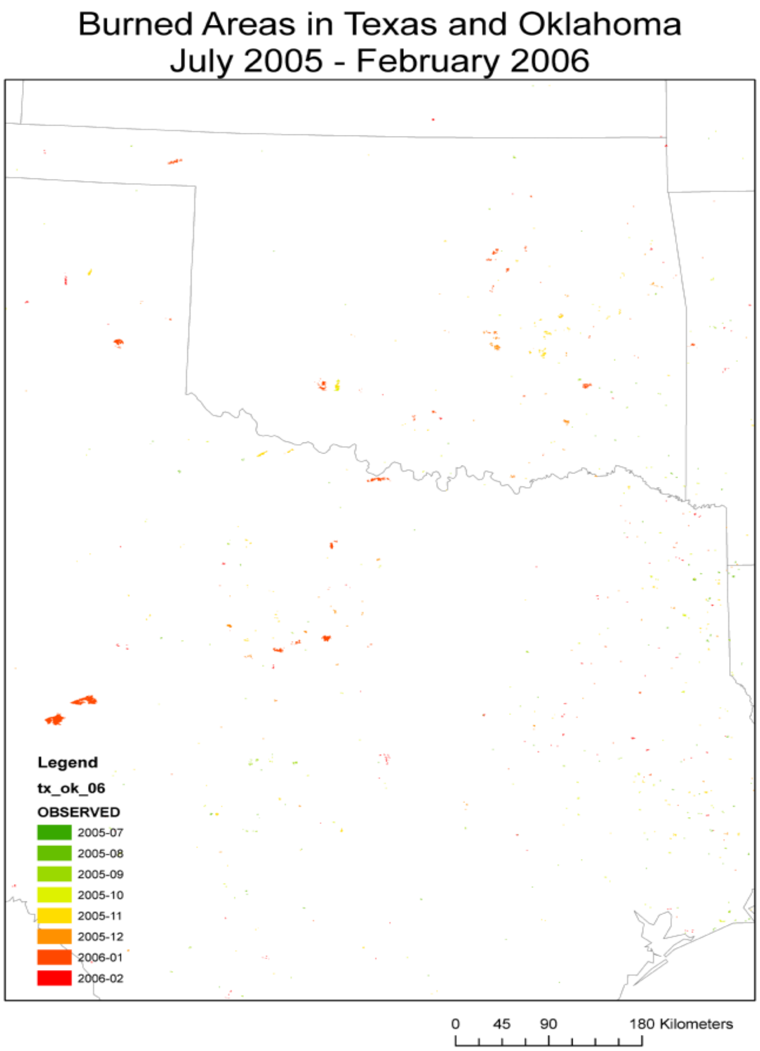

Figure 11: Burned Areas in Texas and Oklahoma: July, 2005 - February 2006

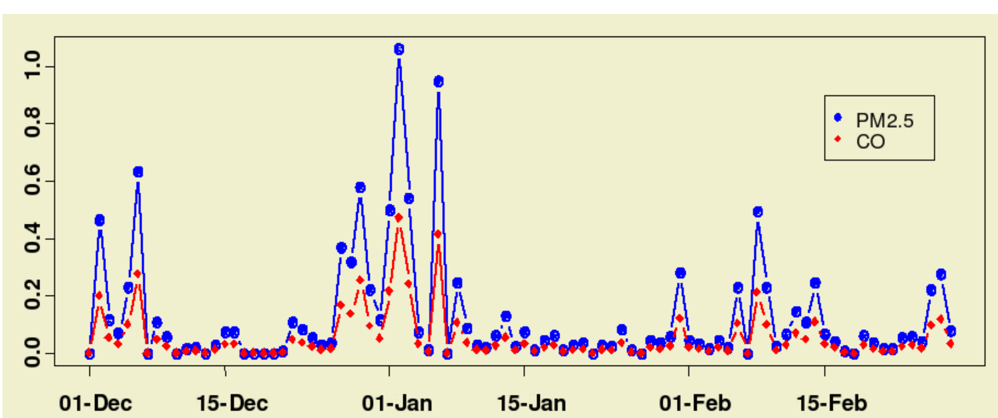

Figure 12: Ratio of fire emissions to anthropogenic emissions for two species over Oklahoma and Texas

7 Transport of Emissions

7.1 Development of HYSPLIT/Chem

The HYSPLIT transport model has been augmented with the Carbon Bond-IV (CB-IV) photochemical mechanism. This version of HYSPLIT (HYSPLIT/Chem) was used to forecast ozone concentrations in the New England 2002 Forecasting Pilot Program. HYSPLIT/Chem, which was parallelized for this effort, has since been refined and optimized for use on a clustering environment which uses the Message Passing Interface (MPI) as a distributed memory model. The fire science lab has acquired and installed a Cray XD1 Linux cluster on which HYSPLIT/Chem is installed. HYSPLIT/Chem compiles and the test case provided by NOAA/ARL runs. The successful completion of these preliminary development steps was prerequisite to the ongoing air quality modeling effort at the Missoula Fire Science Laboratory.

HYSPLIT/Chem has not yet been integrated with the rest of the smoke dispersion system. This is scheduled for the winter of 2006/7. Currently, emissions transport is performed by the Weather Research and Forecasting model with chemistry (WRF/Chem). For the 2007 fire season, the fire science lab's smoke dispersion website will provide smoke trajectories (calculated by HYSPLIT/Chem) as well as smoke coverages (calculated with the aerosol mechanism embedded within WRF/Chem.)

7.2 Transport with WRF/Chem

The methods derived for spatially explicit, satellite-derived emissions computations have a general utility beyond the initially proposed system. They may be aggregated into annual inventories, summarized by incident name, or transported by alternate models. In the system originally proposed, HYSPLIT/Chem was to be used as the transport mechanism. However, the emissions once computed may be assimilated by any chemical transport model. Our operational system uses WRF/Chem as the first chemical transport model due to the inclusion of full aerosol chemistry.

Figure 13 demonstrates the web presentation of concentration forecasts which has been established for use with the WRF/Chem model. This map provides the ability to pan and zoom to the desired region of interest. It provides access to several quantities of interest without clutter. This web presentation is built using open source geospatial software which is being adapted to handle four dimensional data without external help—a task far beyond the scope of “normal” mapping software. Handling four dimensional data will be required by any forecasting system, including one which uses HYSPLIT/Chem. It is expected that the use of HYSPLIT/Chem will require no significant map or data server development effort.

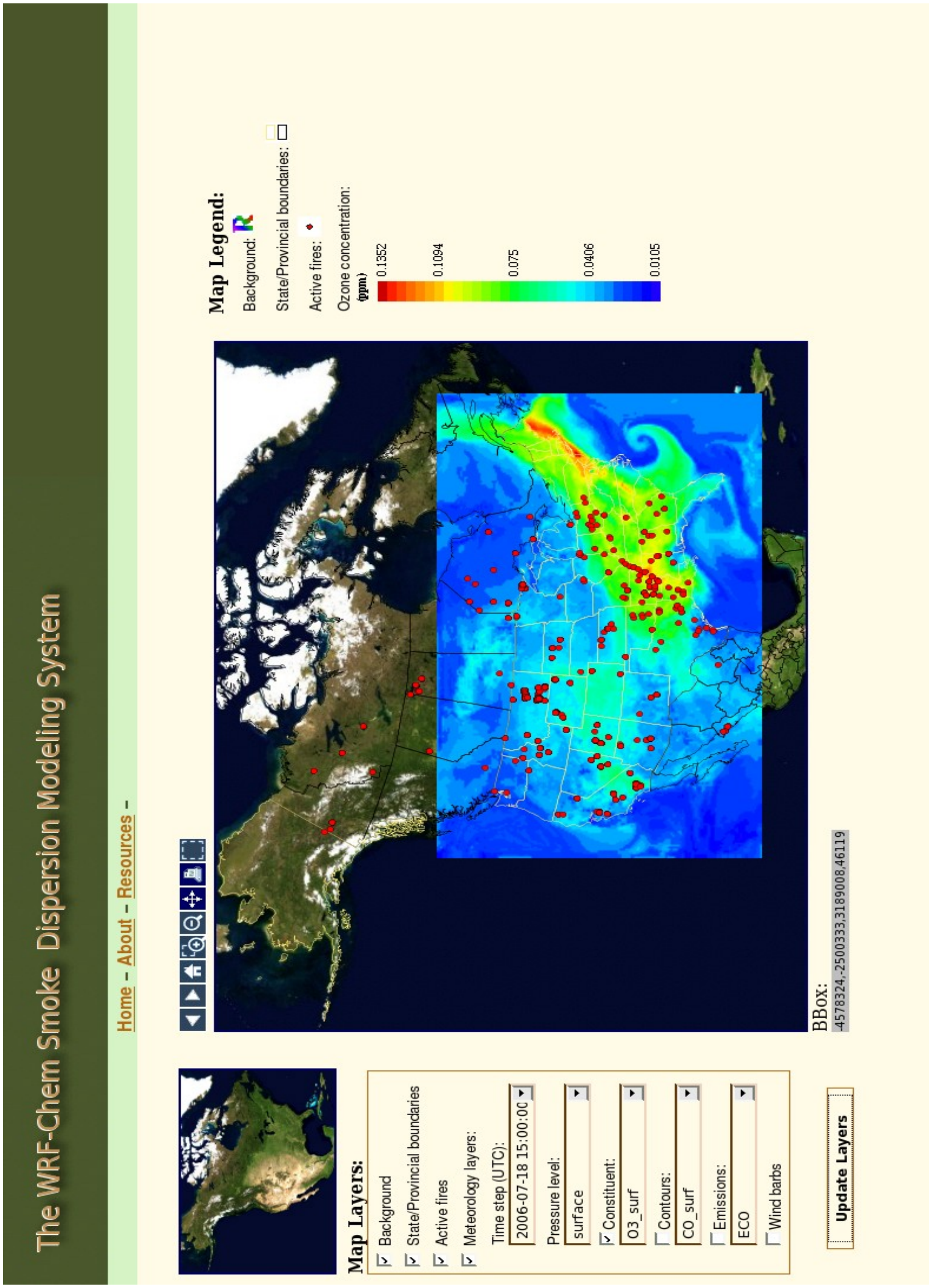

Figure 13: Web presentation of smoke dispersion modeling data.

8 Deliverables

Proposed	Accomplished/Status
An automated forecasting system on smoke dispersion and pollutant levels will be the principal product of this project.	Accomplished. Developmental website URL: http://smoke-fire.us:8080/geoserver/data/quickWMS/alex_devel.jsp
This project will provide locations of active fires, burned areas, and aerosol optical thickness at 10:30 a.m. and 1:30 p.m. daily with 1 km x 1 km resolution in the continental U.S.	Active fires and burned areas are provided as point locations rather than as a 1km x 1km grid at the above website. Aerosol Optical Thickness is not computed. The 1km x 1km AOT algorithm is not yet available from NASA.
A nationwide emissions inventory of pollutants from fires will be computed twice daily.	The current map of fuel emissions is available on the above website for CO and PM2.5.
None	Fuel map of CONUS for use with FOFEM reference database has been produced.
None	Our geospatial processing and display work has been incorporated into the GeoTools java library and the GeoServer web map server. These technologies allow us and others to interact with and render the multidimensional datasets associated with weather models. These capabilities are of generic interest and are available for anyone to use.
None	As part of this effort, we have begun a restructuring of the FARSITE fire behavior simulator. This is intended to be a multi-use code base which can be leveraged by desktop and web applications as well as from the Linux command line.

9 Future Work

1. Integrate HYSPLIT
2. Incorporate FARSITE
3. Incorporate plume rise calculatons.
4. Devise a standard method for fire incident information interchange.

References

[1] Eyre, F. H., 1980, Forest Cover Types of the United States and Canada, Society of American Foresters. Washington D.C.

[2] Giglio, Louis, Jacques Descloitres, Christopher Justice, Yoram Kaufman, 2003, "An Enhanced Contextual Fire Detection Algorithm for MODIS." Remote Sensing of Environment, 87:273-282

[3] Kaufman, Yoram and Chris Justice, Algorithm Theoretical Background Document: MODIS Fire Products, Nov 1998. EOS ID #2741
[4] Kaufman, Yoram, Christopher Justice, Luke Flynn, Jackie Kendall, Elaine Prins, Louis Giglio, Darold Ward, W. Paul Menzel, and Alberto Setzer. December 1998. "Potential global fire monitoring from EOS-MODIS." Journal of Geophysical Research. Vol. 103 No. D24 pp. 32215-32238
[5] Li, Rong-Rong, Y. Kaufman, W. M. Hao, J. M. Salmon, and B.-C. Gao. June 2004. "A Technique for Detecting Burn Scars Using MODIS Data." IEEE Transactions on Geoscience and Remote Sensing. Vol. 42 No. 6 pp. 1300-1308
[6] McKenzie, Don. "FCCS Fuelbed map of the Contiguous United States", http://www.fs.fed.us/pnw/fera/research/fuels/fuelbed_mapping.shtml
[7] Reinhardt, E.D., November 2003, "Using FOFEM 5.0 to estimate tree mortality, fuel consumption, smoke production and soil heating from wildland fire", In: Proceedings of the Second International Wildland Fire Ecology and Fire Management Congress and Fifth Symposium on Fire and Forest Meteorology. American Meteorological Society.
[8] Shiflet, T.N., 1994, Rangeland Cover Types of the United States, Society for Range Managment. Denver, CO
[9] USDA Forest Service. "Wildland Fire Assessment System", http://www.wfas.net
[10] USDA Forest Service. "Fuel Characteristic Classification System", http://www.fs.fed.us/pnw/fera/fccs/index.shtml
[11] USDA Forest Service. "First Order Fire Effects Model", http://www.fire.org